Iranian Journal of Hydrogen & Fuel Cell 2(2021) 103-112

Iranian Journal of Hydrogen & Fuel Cell

IJHFC

Journal homepage://ijhfc.irost.ir

Comparison of waste heat recovery from a Proton Exchange Membrane fuel cell by gas turbine or Organic Rankin Cycle: a display of 3E analysis

Vahid mohammadzadeh[1,3], Fathollah Ommi[2], Zoheir Saboohi[1*], Ehsan Gholamian[4]

[1] Khayyam Research Institute, Ministry of Science, Research, and Technology
[2] Department of Mechanical Engineering, Tarbiat Modares University
[3] Department of Aerospace Engineering, Urmia University of Technology
[4] School of Mechanical Engineering, College of Engineering, University of Tehran, Tehran, Iran

Article Information

Article History:

Received:
13 Jul 2021
Received in revised form:
13 Sep 2021
Accepted:
03 Oct 2021

Keywords

PEM
Fuel cell
ORC
waste heat recovery
hybrid PEMFC/GT

One of the most important methods for efficient hydrogen utilization is the proton exchange membrane fuel cell (PEMFC) because of its low environmental impact and easy maintenance. Depletion of fossil fuels along with global warming is all the more reason for researchers to seek new methods to convert primary energy into power, heating, etc. In the meantime, fuel cells are a promising method to convert energy into usable power. In this study, a proton exchange membrane fuel cell utilizing hydrogen as a fuel is proposed as the main component of a power generation system. The waste heat of the fuel cell is then recovered via two scenarios, using the waste heat as the heat source of an organic Rankin cycle (ORC) or using it to be expanded in the gas turbine. A comprehensive energy and exergy analysis are carried out to find the effectiveness of the system along with the adverse conditions of the components. Results demonstrate that at operation conditions, the system integrated with a gas turbine performs better in terms of energy and exergy efficiencies by 45% and 33%, respectively. Also, Fuel cell, and afterburner has the highest exergy destruction ranks amongst other elements, since they have all three main source of irreversibility. Furthermore, the economic study results show that the PEMFC/GT has a lower Levelized cost of electricity compared to the PEMFC/ORC.

1. Introduction

Nowadays, renewable energies are more attractive than fossil fuels because the latter leads to pollution and greenhouse emissions. The rapid population rise and growing energy need have urged researchers to find solutions that are environment-friendly and highly effective. Fuel cells are a promising method to convert primary energy into power by a very simple and reliable method [1]. Among the different kinds of fuel cells, the proton exchange membrane fuel cell (PEMFC) has attracted lots of attention due to its short start-up time, lower weight, and flexibility in coupling with other energy systems in CHP plants [2]. Boettner and Moran [3] investigated a methanol-reforming PEMFC in a comparative study. Their result

*Corresponding author. saboohi@ari.ac.ir

doi: 10.22104/IJHFC.2021.5062.1227

included both energy and exergy analysis. They found out that a methane-fueled PEMFC has higher exergy destruction than the hydrogen-fueled one. Also, they concluded that increased current density leads to lower effectiveness and voltage in either scenario. Investigation of energy and exergy aspects of a hydrogen-fueled PEM fuel cell at different pressure, flow rate, and voltage values was carried out by Taner [4]. The results designated that the exergy and energy efficiencies become 50.4% and 47.6%, correspondingly. Furthermore, they concluded that higher voltage leads to higher efficiency in a trade-off with lower fuel cell life. Two configurations of vehicular PEM fuel cell systems (with and without an expander) from an exergoeconomic point-of-view were compared by Sayadi et al. [5]. Moreover, due to their reliability, easy maintenance, and economic feasibility, the organic Rankine cycle (ORC) is one of the best candidates to recover the low-temperature waste heat of energy systems (e.g., PEM fuel cells as well as solar thermal and geothermal based energy systems) and convert it into power [6]. Behzadi et al. [7] studied the integration of ORC systems into Tehran's waste-to-energy power plant. Their study included exergy, economic evaluations, and the optimum conditions leading to total product unit cost, and they found the exergy efficiency is 24.65 $/GJ and 19.61%, respectively. The important result was that ORC integration in low-grade heat sources leads to better overall efficiency. Arabkoohsar and Nami [8] researched on hybrid ORC plants. They reported that the efficiency rises from 20% and 10%, and the payback period reduces (from 7.4 years to 6.7 years), respectively, if the hybrid system is integrated. After a comprehensive survey in the literature, it is evident that a comparison of effective waste heat recovery from PEMFC seems necessary. After validation of the results and comprehensive thermodynamic modeling of the system, a parametric study in terms of energy and exergy analysis is performed. In addition, the exergy destruction in different elements of the system is also illustrated.

2. System Description and assumptions

The schematics of the proposed system are illustrated in Figure 1 (a and b). As seen in Figure 1, Fuel enters the fuel compressor and is compressed to state 7. After gaining enough heat to raise its temperature to state 10, the Fuel enters the anode of PEMFC. Air enters the cathode side of PEMFC after being pressurized at the air blower. An electrochemical reaction occurs in the fuel cell, and the power is generated; hot gasses enter the combustion chamber (called the afterburner) to be mixed and burned with the incoming Fuel from the methane compressor. The Exhaust gas at state 12 passes the heat to state 7 and then cools down to state 14. In scenario 1 (Figure 1-a), state 14 enters the GT to generate the power. In scenario 2 (Figure 1-b), state 14 is discharged to the atmosphere, and the heat is used to generate the working fluid to enter the ORC turbine.

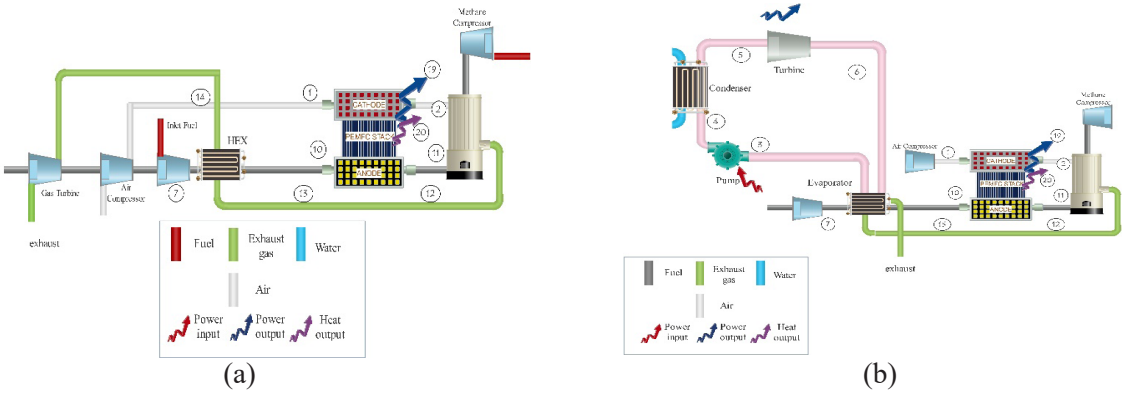

(a) (b)

Fig.1. Schematics of the proposed integrated system.

3. Modeling

In order to carry out a complete technical analysis of the proposed system, each component in the system is considered a control volume and the balance equations (as mass, energy, and exergy) are written as below, respectively [9]

$$\sum \dot{m}_{in} = \sum \dot{m}_{out} \quad (1)$$

$$\dot{Q} - \dot{W} = \sum \dot{m}_{out} h_{out} - \sum \dot{m}_{in} h_{in} \quad (2)$$

$$\dot{E}_Q - \dot{E}_W = \sum \dot{m}_{out} e_{out} - \sum \dot{m}_{in} e_{in} + \dot{E}_D \quad (3)$$

Where Q and W denote the rate of heat and power crossing the control volume surface. In the systems where the chemical reaction occurs, the chemical exergy shall be taken into consideration as below [10]:

$$e_i = e_i^{ph} - e_i^{ch} \quad (4)$$

$$e_i^{ph} = (h_i - h_0) T_0 (s_i - s_0) \quad (5)$$

The incoming air to the cathode and the Fuel into the anode undergo a certain set of electrochemical reactions in which the electron is separated from the hydrogen and travels through the electrical circuit to generate the electricity and then goes back into the cathode to reunite with the H^+; these equations are presented below [11]:

Anode: $H_2 \rightarrow 2H^+ + 2e^-$ (6)

Cathode: $2H^+ + 2e^- + \frac{1}{2}O_2 \rightarrow H_2O$ (7)

Overall reaction: $H_2 + \frac{1}{2}O_2 \rightarrow H_2O + W + Q$ (8)

Also, Watts law suggests that the output power of the fuel cell is the product of voltage and current in which is used as a factor to alter DC to AC electricity [11]:

$$W_{PEMFC.DC} = N_c i A V_c \quad (9)$$

$$W_{PEMFC.AC} = W_{PEMFC.DC} \times \eta_{inv} \quad (10)$$

To find the deviation of the cell voltage from Nominal voltage, the losses are subtracted as shown below [11]:

$$V_C = V_N - V_{loss} \quad (11)$$

Where the nernest or nominal voltage is defined as [11]:

$$V_N = 1.229 - 0.85 \times 10^{-3}(T - 298.15) + 4.31 \times 10^{-5} T \left(\ln\left(P_{H_2}\sqrt{P_{O_2}}\right)\right) \quad (12)$$

P_{H_2} and P_{O_2} represent the partial pressure of hydrogen and oxygen, respectively, at the exit of the fuel cell [11, 12]. The sum of losses (as ohmic, activation, and concentration) form the overall loss voltage in the cell:

$$V_{loss} = V_{ohm} + V_{act} + V_{conc} \quad (13)$$

In which V_{ohm} can be determined as:

$$V_{ohm} = IR_{\text{int}} \quad (14)$$

$$I = iA \quad (15)$$

$$R_{\text{int}} = \frac{rM^{l}}{A} \quad (16)$$

Where R_{int} is the internal resistance of the fuel cell [11]. Moreover, the activation polarization in the fuel cell is composed of two sections in the anode and cathode as:

$$V_{act} = -(-0.948 + \zeta T + 7.6\times10^{-5} T \ln(I)) \quad (17)$$

$$\zeta = 0.00286 + 0.0002\ln(A) + 4.38\times10^{-5}\ln(C_{H_2}) \quad (18)$$

$$C_{O_2} = 1.97\times10^{-7} P_{O_2} \exp(\frac{498}{T}) \quad (19)$$

$$C_{H_2} = 9.174\times10^{-7} P_{H_2} \exp(\frac{-77}{T}) \quad (20)$$

Finally, the losses, which are due to the concentrated electrolytes in the cell, is projected as [11]:

$$V_{conc} = \frac{RT}{n_e F}\ln(\frac{i_L}{i_L - i}) \quad (21)$$

The constants in the above equations are duly defined in [12].

According to equation 20, the used up hydrogen and oxygen in the cathode, anode, and produced products (mainly water) can be related to the current passing through the cell as[11]:

$$\dot{n}_{H_2,cons} = \frac{N_c I}{2F} \quad (22)$$

$$\dot{n}_{O_2,cons} = \frac{N_c I}{4F} \quad (23)$$

$$\dot{n}_{H_2O,gene} = \frac{N_c I}{2F} \quad (24)$$

In order to be sure the electrochemical reaction has fully occurred in the PEMFC, the excess hydrogen and oxygen (other than what was defined in Eqs. 34-36) are supplied into the channels of the PEMFC. That amount can be found from the equations below [11]:

$$\dot{n}_{H_2,inl} = \lambda_{H_2}\dot{n}_{H_2,cons} \quad (25)$$

$$\dot{n}_{O_2,inl} = \lambda_{O_2}\dot{n}_{O_2,cons} \quad (26)$$

Unlike the SOFC and MCFC, the PEMFC has a considerable amount of waste heat in the stack that can be used in the organic Rankin cycle; this heat can be determined by [11]:

$$\dot{Q}_{PEMFFC} = \dot{Q}_{ch} - \dot{W}_{PEMFC,DC} - \dot{Q}_{sl} \quad (27)$$

$$\dot{Q}_{ch} = \dot{n}_{H_2,cons}\overline{LHV} \quad (28)$$

$$\dot{Q}_{s,l} = \bar{C}_{P,H_2}(\dot{n}_{H_2,out}T - \dot{n}_{H_2,inl}T_{amb}) + \bar{C}_{P,O_2}(\dot{n}_{O_2,out}T - \dot{n}_{O_2,inl}T_{amb}) + \bar{C}_{P,N_2}(\dot{n}_{N_2,out}T - \dot{n}_{N_2,inl}T_{amb}) + \dot{n}_{H_2O,gene}\bar{H}_v \quad (29)$$

Where the sensible and input heats are denoted by $\dot{Q}_{s,l}$ and $\dot{Q}_{ch}$, respectively.

Also, the exergy balance equations for other system components, e.g., the ORC cycle, heat exchangers, and GT, are shown in Table 1:

Table 1. The exergy Balance expressions for the components of the system.

ORC evaporator	$\dot{E}_{D,ORC\ evap}=(\dot{E}_7-\dot{E}_{10})+(\dot{E}_{13}-\dot{E}_{\text{exhust}})$
ORC condenser	$\dot{E}_{D,ORC\ cond}=(\dot{E}_4-\dot{E}_5)+(\dot{E}_{\text{water,in}}-\dot{E}_{\text{water,out}})$
ORC turbine	$\dot{E}_{D,ORC\ \text{turbine}}=(\dot{E}_5-\dot{E}_6)-\dot{W}_{ORC\ turbine}$
GT	$\dot{E}_{D,GT}=(\dot{E}_{14}-\dot{E}_{15})-\dot{W}_{GT}$
ORC pump	$\dot{E}_{D,ORC\ pump}=\dot{W}_{ORC\ pump}+(\dot{E}_{24}-\dot{E}_{21})$
HEX	$\dot{E}_{D,HEX}=(\dot{E}_7-\dot{E}_{10})+(\dot{E}_{13}-\dot{E}_{14})$
PEMFC	$\dot{E}_{D,PEM}=(\dot{E}_1-\dot{E}_2)+(\dot{E}_{10}-\dot{E}_{11})$
After Burner	$\dot{E}_{D,AB}=(\dot{E}_{11}+\dot{E}_2)-\dot{E}_{12}$

3.1. Economic analysis

The exergoeconomic analysis is formed by a combination of exergy and economic investigation. It provides comprehensive information about the Fuel and product of a system that is not available from only exergy or economic analysis. Hence, the unit product cost can be considered a suitable objective function in investigating systems optimization. The exergoeconomic balance equation for each system component is expressed as below:

$$\sum C_{k.in}\dot{E}_{k.in}+C_{q.k}\dot{E}_k+\dot{Z}_k=\sum C_{k.out}\dot{E}_{k.out}+C_{w.k}\dot{E}_{w.k} \quad (30)$$

In the above equation, c and $\dot{Z}_k$ are related to per exergy unit cost and components cost in per hour that can be find from following equation :

$$\dot{Z}_k=\frac{Z_k.CRF.\varphi}{\tau} \quad (31)$$

The formula of total investment cost for components is listed in Table 3. Moreover, τ, φ, show the annual operating hours and maintenance factor, respectively, of 8000h and 0.06 [16]. The capital recovery factor (CRF) also is calculated from Eq. 41:

$$CRF=\frac{i(1+i)^n}{(1+i)^n-1} \quad (32)$$

Where *n* shows the lifetime of cycle, and *i* indicates the interest rate. Eventually, to convert the calculated cost to the present cost, the below equation is applied [13]:

$$\text{cost at present year}=\text{Origen cost}\times\frac{\text{cost index for the present year}}{\text{cost index for the year of original cost}} \quad (33)$$

The values of $\dot{Z}_k$ can be found in literature [14].

3.2. Performance evaluation

The comparison and assessment of the system in terms of energy and exergy is vital to evaluate the working conditions. So, net output power, overall energy, and exergy efficiencies are calculated as follows, respectively:

$$\eta_I=\frac{\dot{W}_{net}+\dot{W}_{GT/ORC}}{\dot{m}_{Fuel}LHV_{Fuel}} \quad (34)$$

$$\eta_{II}=\frac{\dot{W}_{net}+\dot{W}_{GT/ORC}}{\dot{E}_{in}} \quad (35)$$

Where $\dot{W}_{net}$ is the net power output of the entire system in either case and can be found by:

$$\dot{W}_{net}=\dot{W}_{PEMFC,AC}+\dot{W}_{Gas\ \text{turbine}}/(\dot{W}_{ORC\ \text{turbine}}-\dot{W}_{ORC\ pump}) \quad (36)$$

4. Results and Discussion

Validation of the results was performed to make sure that the developed model is accurate . To verify the modeling outcomes of the PEM fuel cell, the results reported by Chen *et al*. [15] and Tu *et al*. [16] are compared to those acquired by the present model, see *Table 2*.

Table 2. Comparison of the output voltage of the PEM fuel cell obtained from the present model with data reported by Chen et al. [15] and Tu et al. [16].

Inlet gas temperature (K)	Output voltage (V)		
	Present model	Chen et al. [15]	Tu et al. [16]
348	0.657	0.656	0.655
353	0.681	0.678	0.678
358	0.693	0.691	0.690

Before beginning the simulation an input data table is given as in Table 3.

Table 3. Input data table.

Parameter	value
PEMFC	
i (A/cm²)	0.6
U_f	0.85
ΔT_{stack} (°C)	5
T_{PEMFC} (K)	353
P_{PEMFC} (bar)	3
A (cm²)	200
N_c	13
η_{inv}	0.97
i_L (A/cm²)	1.5
λ_{H_2}	1.2
λ_{O_2}	2
F (C/mol)	96485
R_{CR}	0.4
L (cm)	0.0178
ψ	7
$\Delta T_{pp,\ evap}$	10
$\eta_{ORC\ pump}$ (%)	0.9
$\eta_{ORC\ turbine}$ (%)	0.85
$P_{inlet\ turbine}$ (kPa)	2500
T_0 (°C)	25
P_0 (kPa)	101.3

A parametric study was conducted to see the effect of different design variables on the integrated system performance. The first parameter to discuss is the fuel utilization factor. Figure 2 illustrates the fuel utilization factor impact on the energy and exergy efficiencies of the system. Figure 2a shows the system with ORC, and 2b utilizes GT. According to these figures, increasing the fuel utilization factor has a diverse effect on the performance of the system, and increasing the value from 0.75 to 0.95 causes the energy and exergy efficiencies of the PEMFC/ORC to decrease by 3.5% and 2%, respectively. Moreover, the system integrated with GT has, on average, 4% more exergy and energy efficiency.

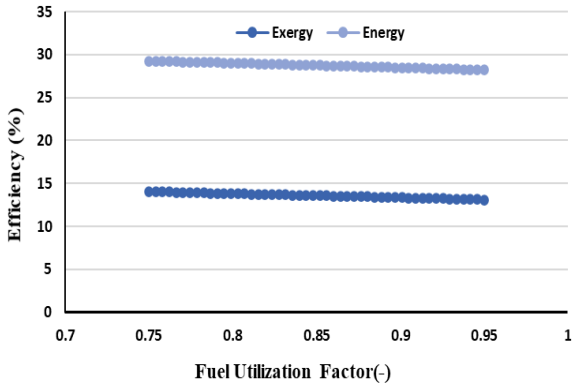

(a)

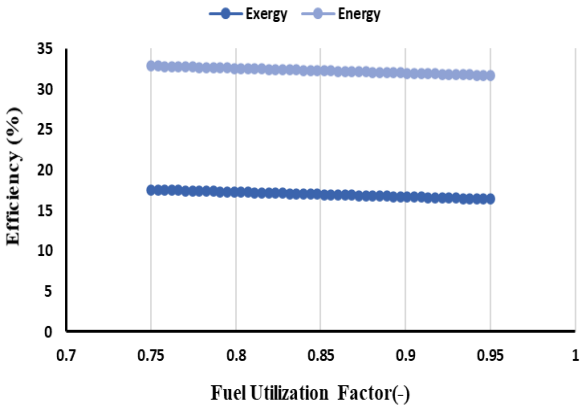

(b)

Fig. 2. The effect of fuel utilization factor on the energy and exergy efficiency of the system.

The effect of current density on the performance indicators of both cycles is depicted in Figure 3. According to this figure, increasing the current density is a good action that results in a 22.5% and 15% increase in energy and exergy efficiency, respectively. Also, using PEMFC/GT is more efficient than PEMFC/ORC.

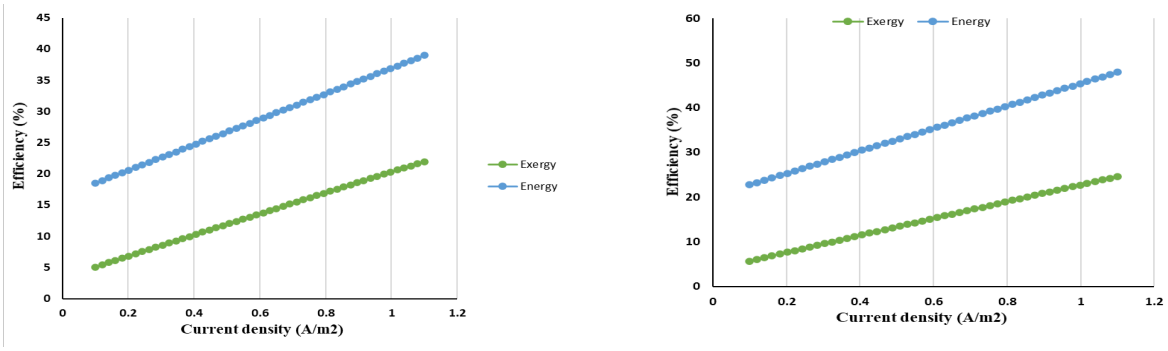

(a) (b)

Fig. 3. The effect of current density on the energy and exergy efficiency of the system.

Another essential factor to discuss is the effect of the stack temperature difference, which is depicted in Figure 4. According to this figure, the inlet temperature is fixed, and the outlet temperature (which is the cell temperature) varies from 2 to 17 °C. The rise in the temperature causes the reaction rate to increase, increasing the generated electrical energy, resulting in an increase in the exergy and energy effectiveness by 7.72% and 3.86% in the case of PEM/GT and 7.48% and 3.75% in the case of PEM/ORC. Moreover, the use of PEM/GT has a higher exergy efficiency of 24.9% at the maximum temperature.

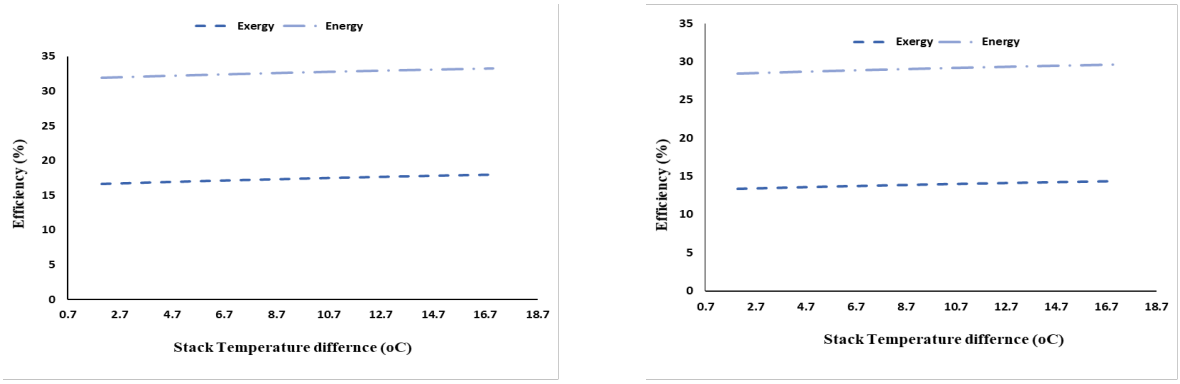

(a) (b)

Fig. 4. The effect of current density on the energy and exergy efficiency of the system.

Figure 5 shows the exergy destruction in the different components of the system and can be used to ascertain the inefficient parts of the system. According to this figure, all three significant sources of irreversibility, which are mixing, temperature difference, and chemical reactions, occur in the fuel cell and afterburner. So, this element has 8.55 kW and 6.10 kW exergy destruction, respectively, which is the highest among all the components.

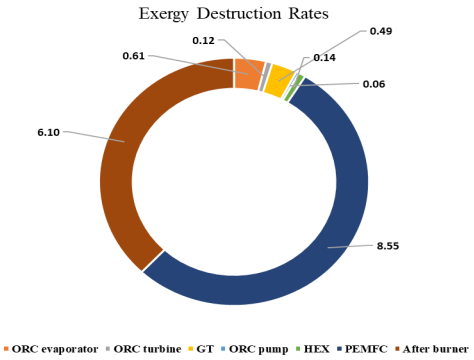

Fig. 5. Exergy Destruction rates in the system components.

4.1. Economic analysis results

When assessing thermal systems, including fuel cells, the economic behavior of the system is a key factor in the decision-making of the designers. In this regard, Figure 6 represents the change in the Levelized cost of electricity with the change in the current density. According to this figure, changing the current density from 0.1 to 1.1 A/cm^2 results in a 77% reduction in the LCOE of the PEMFC/GT. This means that increasing the current density causes the net power of the fuel cell to increase, and since it is in the denominator of the LCOE [17], it causes a reduction in the LCOE.

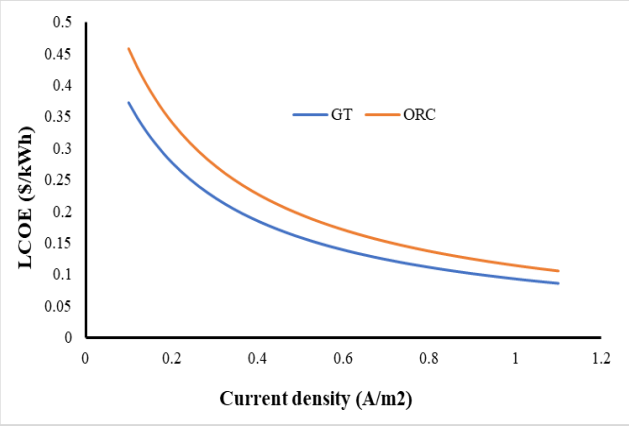

Fig. 6. Variation of Levelized cost of electricity with current density for PEMFC/GT and PEMFC/ORC.

Figure 7 also depicts the effect of the fuel utilization factor on LCOE. According to this figure, increasing the fuel utilization factor works opposite from the LCOE and causes a 7% increase in the cost in PEMFC/GT. This is because an increase in the fuel flow rate results in a slight decrease in the net power of the fuel cell, and the LCOE in the ORC case is 23% higher than PEMFC/GT.

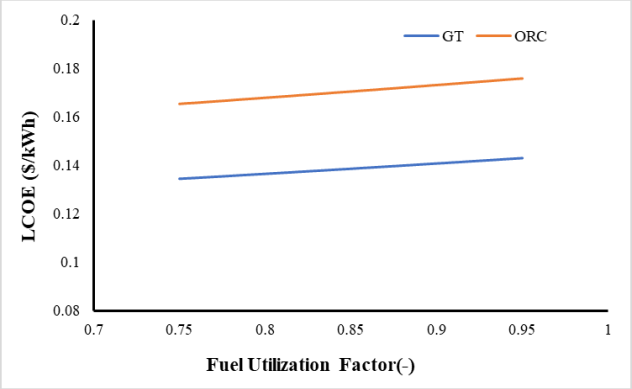

Fig. 7. Variation of Levelized cost of electricity with Fuel Utilization factor for PEMFC/GT and PEMFC/ORC.

The last but not the least important figure to discuss here is the temperature at which the electrochemical reaction occurs, namely, stack temperature difference. According to Figure 8, the increase in stack temperature difference causes a reduction of nearly 6% in the LCOE of the PEM/GT and PEM/ORC. The cost of the PEMFC/GT at higher operating temperatures is lower than that of the PEMFC/ORC, as anticipated.

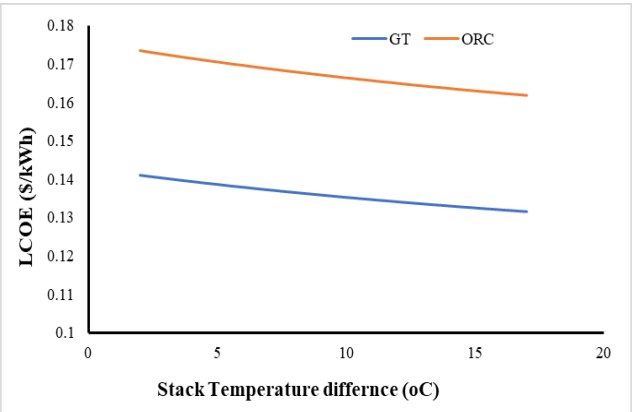

Fig 8. Variation of Levelized cost of electricity with Stack Temperature difference for PEMFC/GT and PEMFC/ORC.

5. Conclusion

In this research article, the importance of fuel cells is discussed, and the importance of this study is illustrated. In this study, a comparison is made between two compelling scenarios to exploit the waste heat of PEMFC with either GT or an ORC. Comprehensive modeling of the energy, exergy, and economic assessments of the system was carried out. The effective parameters of the system were also studied by parametric analysis. Results show that the PEMFC and afterburner have the highest exergy destruction rates of 8.55 kW and 6.10 kW, respectively, in the whole system. The Parametric study revealed that the fuel utilization factor, current density, stack temperature difference, and turbine inlet temperature have the greatest effect on system performance criteria. It is indicated that the PEMFC/GT has higher capabilities than the PEMFC/ORC. Also, increasing fuel utilization factor harms the efficiency, but increasing current density is favorable to the system. The economic analysis illustrates that the system with PEMFC/GT is a more economically viable option to generate power, and the LCOE reaches nearly 0.1 $/kWh at design conditions.

References

[1] Moradi M, Mehrpooya M. Optimal design and economic analysis of a hybrid solid oxide fuel cell and parabolic solar dish collector, combined cooling, heating and power (CCHP) system used for a large commercial tower. Energy 2017;130:530–43. https://doi.org/10.1016/j.energy.2017.05.001.

[2] Dashti I, Asghari S, Goudarzi M, Meyer Q, Mehrabani-Zeinabad A, Brett DJL. Optimization of the performance, operation conditions and purge rate for a dead-ended anode proton exchange membrane fuel cell using an analytical model. Energy 2019;179:173–85. https://doi.org/10.1016/J.ENERGY.2019.04.118.

[3] Boettner DD, Moran MJ. Proton exchange membrane (PEM) fuel cell-powered vehicle performance using direct-hydrogen fueling and on-board methanol reforming. Energy 2004;29:2317–30. https://doi.org/10.1016/j.energy.2004.03.026.

[4] Taner T. Energy and exergy analyze of PEM fuel cell: A case study of modeling and simulations. Energy 2018;143:284–94. https://doi.org/10.1016/j.energy.2017.10.102.

[5] Sayadi S, Tsatsaronis G, Duelk C. Exergoeconomic analysis of vehicular PEM (proton exchange membrane) fuel cell systems with and without expander. Energy 2014;77:608–22. https://doi.org/10.1016/j.energy.2014.09.054.

[6] Yu H, Eason J, Biegler LT, Feng X. Simultaneous heat integration and techno-economic optimization of Organic Rankine Cycle (ORC) for multiple waste heat stream recovery. Energy 2017;119:322–33. https://doi.org/10.1016/j.energy.2016.12.061.

[7] Behzadi A, Gholamian E, Houshfar E, Habibollahzade A. Multi-objective optimization and exergoeconomic analysis of waste heat recovery from Tehran's waste-to-energy plant integrated with an ORC unit. Energy 2018;160:1055–68. https://doi.org/10.1016/j.energy.2018.07.074.

[8] Arabkoohsar A, Nami H. Thermodynamic and economic analyses of a hybrid waste-driven CHP–ORC plant with exhaust heat recovery. Energy Convers Manag 2019;187:512–22. https://doi.org/10.1016/J.ENCONMAN.2019.03.027.

[9] Arabkoohsar A, Machado L, Farzaneh-Gord M, Koury RNN. The first and second law analysis of a grid connected photovoltaic plant equipped with a compressed air energy storage unit. Energy 2015;87:520–39. https://doi.org/10.1016/j.energy.2015.05.008.

[10] Nami H, Arabkoohsar A. Improving the power share of waste-driven CHP plants via parallelization with a small-scale Rankine cycle, a thermodynamic analysis. Energy 2019;171:27–36. https://doi.org/10.1016/j.energy.2018.12.168.

[11] Baniasadi E, Toghyani S, Afshari E. Exergetic and exergoeconomic evaluation of a trigeneration system based on natural gas-PEM fuel cell. Int J Hydrogen Energy 2017;42:5327–39. https://doi.org/10.1016/J.IJHYDENE.2016.11.063.

[12] Behzadi A, Arabkoohsar A, Gholamian E. Multi-criteria optimization of a biomass-fired proton exchange membrane fuel cell integrated with organic rankine cycle/thermoelectric generator using different gasification agents. Energy 2020;201:117640. https://doi.org/10.1016/J.ENERGY.2020.117640.

[13] Fakhari I, Behzadi A, Gholamian E, Ahmadi P, Arabkoohsar A. Comparative double and integer optimization of low-grade heat recovery from PEM fuel cells employing an organic Rankine cycle with zeotropic mixtures. Energy Convers Manag 2021;228:113695. https://doi.org/10.1016/j.enconman.2020.113695.

[14] Behzadi A, Arabkoohsar A, Gholamian E. Multi-criteria optimization of a biomass-fired proton exchange membrane fuel cell integrated with organic rankine cycle/thermoelectric generator using different gasification agents. Energy 2020;201:117640. https://doi.org/10.1016/J.ENERGY.2020.117640.

[15] Chen X, Gong G, Wan Z, Luo L, Wan J. Performance analysis of 5 kW PEMFC-based residential micro-CCHP with absorption chiller. Int J Hydrogen Energy 2015;40:10647–57. https://doi.org/10.1016/j.ijhydene.2015.06.139.

[16] Tu Z, Zhang H, Luo Z, Liu J, Wan Z, Pan M. Evaluation of 5 kW proton exchange membrane fuel cell stack operated at 95 C under ambient pressure. J Power Sources 2013;222:277–81. https://doi.org/10.1016/j.jpowsour.2012.08.081.

[17] Behzadi A, Gholamian E, Houshfar E, Habibollahzade A. Multi-objective optimization and exergoeconomic analysis of waste heat recovery from Tehran's waste-to-energy plant integrated with an ORC unit. Energy 2018;160:1055–68. https://doi.org/10.1016/J.ENERGY.2018.07.074.